Available online at www.sciencedirect.com
ScienceDirect
International Journal of Heat and Fluid Flow 27 (2006) 1069–1077
International Journal of HEAT AND FLUID FLOW
www.elsevier.com/locate/ijhff

Microfluidic characteristics of a multi-holed baffle plate micro-reactor

Behdad Moghtaderi [a,*], Iman Shames [c], L. Djenidi [b]

[a] Discipline of Chemical Engineering, School of Engineering, Faculty of Engineering and Built Environment, The University of Newcastle, University Drive, Callaghan, NSW 2308, Australia
[b] Discipline of Mechanical Engineering, School of Engineering, Faculty of Engineering and Built Environment, The University of Newcastle, University Drive, Callaghan, NSW 2308, Australia
[c] Department of Electrical Engineering, Faculty of Engineering, Shiraz University, Iran

Received 20 January 2005; received in revised form 9 February 2005; accepted 19 January 2006
Available online 2 May 2006

Abstract

As part of a larger project aiming at development of a miniaturized hydrogen generator for small mobile/onboard fuel cell applications, a series of experiments was conducted on a novel micro-reactor to examine the effectiveness of its design in promoting the mixing of reactant agents. The reactor is essentially a tubular vessel fitted with a multi-holed baffle plate mounted on a central tube. The mixing phenomenon within the micro-reactor was studied using the micro-PIV (micro-particle image velocimetry) flow visualization technique. Experiments were conducted on a 1:1 scale replica of the reactor. Results indicate that the application of the multi-holed baffle plate considerably improves the mixing performance of the reactor when compared with a simpler co-axial jet tubular reactor. However, the geometrical characteristics of the baffle plate and central tube are found to have dramatic impacts upon the flow structure and mixing patterns within the reactor. Hence, the optimization of the reactor geometry is required to achieve the desirable mixing performance. For the range of Reynolds numbers studied here, the optimum reactor geometry is achieved when the central tube and baffle holes are of similar diameters and baffle holes are located half way between the stream-wise axis and the reactor wall.

Keywords: Microfluidics; Micro-reactor; Micro-PIV

1. Introduction

Hydrogen is viewed by many scientists as a key element of the sustainable energy scenarios of the future (Winter, 2004) primarily because hydrogen is a clean fuel (i.e., oxidation of hydrogen generates only water) with an extremely high energy content. In fact, the energy storage density of hydrogen is about 120 MJ/kg, whereas the state-of-the-art lithium ion batteries used in common electronic systems, such as cell phones and notebook computers provide about 0.5 MJ/kg. Thus even a very low efficiency hydrogen powered system with about 5% thermal-to-electrical conversion efficiency would be 12 times more powerful than a conventional battery powered system. However, hydrogen is considered as a secondary source of energy because it cannot be found in its pure form on earth despite the fact that hydrogen is among the most abundant elements on our planet (Penner, 2004). As a results, hydrogen should be either generated from a primary energy resource, such as fossil fuels and renewable energy sources, or be produced in nuclear reactors by applying the waste heat to dissociate water.

Once generated, the hydrogen can be utilized in fuel-cells to produce heat and power through a highly efficient oxidative conversion process. The success of fuel cells, however, greatly depends on the availability of suitable

* Corresponding author. Tel.: +61 2 4921 6183; fax: +61 2 4921 6920.
E-mail address: Behdad.Moghtaderi@newcastle.edu.au (B. Moghtaderi).

0142-727X/$ - see front matter © 2006 Elsevier Inc. All rights reserved.
doi:10.1016/j.ijheatfluidflow.2006.01.008

technologies for safe and efficient production of hydrogen. Among various alternatives, partial oxidation of methane (POM) is an attractive option because the reaction is extremely fast, particularly, at high temperatures and methane is readily available in many parts of the world. Miniaturization of this process will further improve the attractiveness of the POM technology particularly for small mobile/onboard applications, such as electrical and electronic devices, and cars (Wegeng et al., 2001). This is not only due to the light weight and suitable physical dimensions of the resulting hydrogen generator but also because of the typical heat and mass transport intensifications achieved in micro-reactors (Tiggelaar et al., 2004; Fletcher et al., 2002; Ehrfeld et al., 2000; Nguyen and Wereley, 2002). There are several reasons for the enhancement of heat and mass transfer processes in micro-reactors, including:

- their smaller dimensions increase the respective gradients of temperature, concentration, and density by several orders of magnitude intensifying the heat and mass transfer processes, and;
- their larger surface-to-volume-ratios provide substantial contact area between reactants, hence, notably decreasing the residence time.

In addition the smaller volumes of micro-reactors decrease the material hold-up resulting in an increase in the process safety while allowing a typical batch-process to be replaced by continuous operation.

Unfortunately, micro-reactors often have poor mixing efficiencies as they generally operate under laminar flow conditions owing to their small physical dimensions. The mixing within these reactors is principally due to molecular diffusion rather than the bulk flow mixing due to turbulence (Ehrfeld et al., 2000; Nguyen and Wereley, 2002). Therefore, better mixing efficiencies within micro-reactors are always desirable. For this reason, numerous researchers have been working on various methods of enhancing the mixing phenomenon in micro-rectors over the last decade. Excellent summaries of these works are provided by Ehrfeld et al. (2000) and Nguyen and Wereley (2002).

According to the literature, of the mixing enhancement methods available today the so-called "Streaming Mixing" techniques are of particular interest in microfluidics because the enhanced mixing can be achieved by proper design of the reactor geometry without the need for mechanical agitation.

Several proven Streaming Mixing strategies (Ehrfeld et al., 2000; Nguyen and Wereley, 2002) have been integrated in the design of the micro-reactor discussed in this study (Fig. 1) providing it with a flexible and robust platform for mixing at micro-scale levels. The Streaming Mixing strategies employed here include contacting, splitting/recombination, and velocity increase. Contacting of the reactant streams is achieved by using a co-axial jet configuration while the velocity-increase and splitting/recombination are attained by employing a multi-holed baffle plate. This configuration also facilitates the task of parallelization of the reactor with an appropriate number of identical reactor units to achieve the required overall production rate. Woodfield et al. (2003) numerically studied the flow characteristics of a micro-can combustor with a similar geometry to that used here for the micro-reactor. However, no experimental measurements were provided by these researchers to verify their numerical predictions. Choi et al. (2002) also experimentally studied the mixing and burning performance of a micro-can combustor similar to that employed in Woodfield et al. (2003) study. Although, their reactor was fitted a multi-nozzles system comprising several nozzles as large as few millimeters in diameter. The difference in size and geometry of the inlet system, made it difficult to draw any quantitative conclusions from Choi's work and apply it to the micro-reactor under investigated in our study.

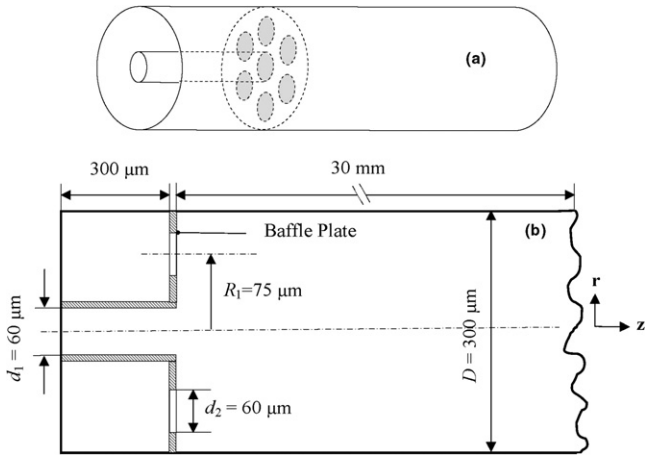

Fig. 1. Schematic illustration (not to scale) of the micro-reactor model: (a) perspective view and (b) side view.

The aim of the study presented in this paper was to examine the microfluidic (i.e., micro-scale fluid dynamic) characteristics of the micro-reactor shown schematically in Fig. 1 for integration into a miniaturized hydrogen generator being developed by the authors at the University of Newcastle, Australia, based on the POM concept. The prototype of the hydrogen generator has about 2500 micro-reactors (similar to that shown in Fig. 1) which have been arranged in 32 reactor plate assemblies each comprising 78 micro-reactors in parallel. The most innovative feature of the micro-reactor depicted in Fig. 1 is that it provides a flexible and robust platform for mixing at micro-scale levels by integrating several proven Streaming Mixing strategies, such as contacting, splitting/recombination, and velocity increase, into a unified system. Contacting of the reactant streams is achieved by using the co-axial jet configuration while the velocity-increase and splitting/recombination are attained by employing the multi-holed baffle plate. This configuration also facilitates the task of parallelization of the reactor with identical reactor units to achieve the required overall production rate.

The focus of our research was on the effectiveness of the reactor design in terms of the mixing behavior of reactant streams. This was achieved by obtaining detailed information on the flow field and velocity distribution in a model reactor using a laser based flow visualization technique known as micro-PIV (micro-particle image velocimetry). The ultimate goal was to improve the design and help develop new strategies for enhancing the mixing within the micro-reactor.

It should be emphasized here that the work presented in this article is an attempt to understand the fluid mechanics of the micro-reactor under cold flow conditions (no heat generation). The heat generation and the subsequent transfer of heat might have some impact on the microfluidics characteristics of the reactor. This issue is the subject of our future studies.

2. Methods and techniques

2.1. Micro-reactor model

The micro-reactor model studied here is essentially a 1:1 scale replica of the actual reactor comprising a tubular vessel fitted with a fuel inlet tube, located co-axially in the main vessel, and a multi-holed baffle plate through which the oxidizing agent is introduced. The reactor has an inside diameter of 300 μm and is 30 mm long. Other dimensions including the inside diameters of the baffle holes (60 μm) and the fuel inlet tube (60 μm) are presented in Fig. 1.

The main vessel was fabricated by wet etching of fused silica (glass) wafers using a solution of NHO_3. For this purpose two identical channels, each representing half of the final assembly, were etched in glass wafers using a polysilicon mask (Sobek et al., 1994). Three access channels were also etched in the glass wafers for delivery of fuel and oxidizer streams from their respective access holes (see Fig. 2(a)). The baffle plate and the fuel inlet tube were fabricated as separated units by cutting to shape small blocks of glass using the Laser Ablation Micromachining technique. The fuel inlet tube and the baffle plate were then glowed together and the assembly was glowed into the channel etched in one of the glass wafers. The two glass wafers were next bonded together at high temperatures to make the final structure.

Fig. 2(b) provides the microscopic top view of one of the glass wafers fitted with the baffle plate/fuel inlet tube

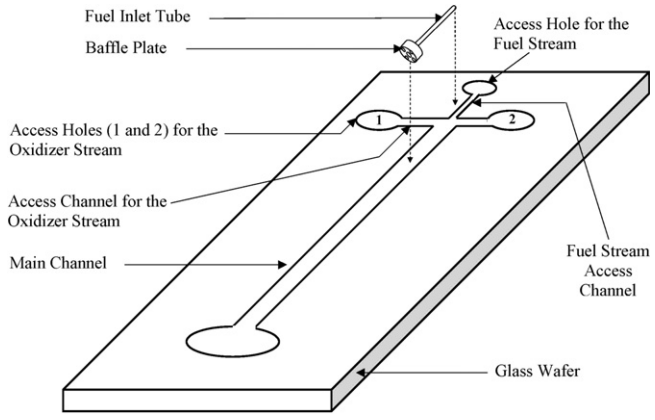

Fig. 2(a). Schematic representation of a glass wafer showing access holes and channels for both fuel and oxidizer streams.

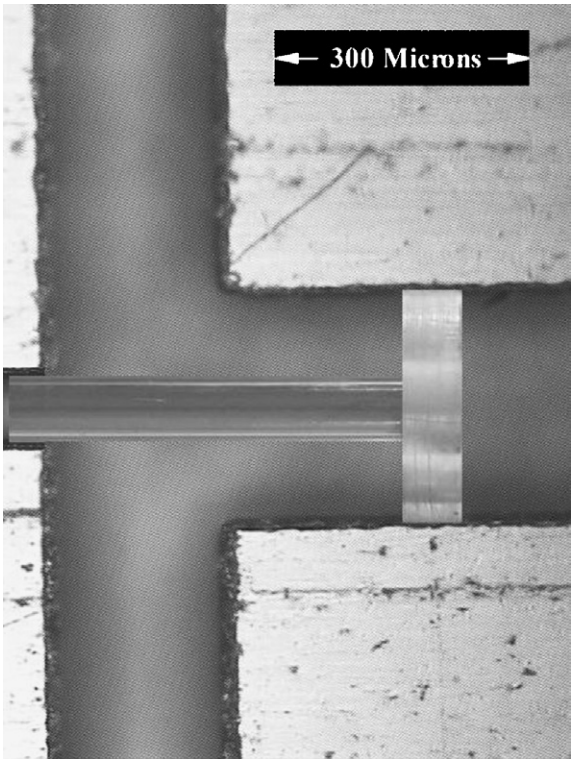

Fig. 2(b). Microscopic top view of a glass wafer fitted with the baffle plate/inlet tube assembly. This picture shows the region near the base of the micro-reactor. Access channels are quite visible.

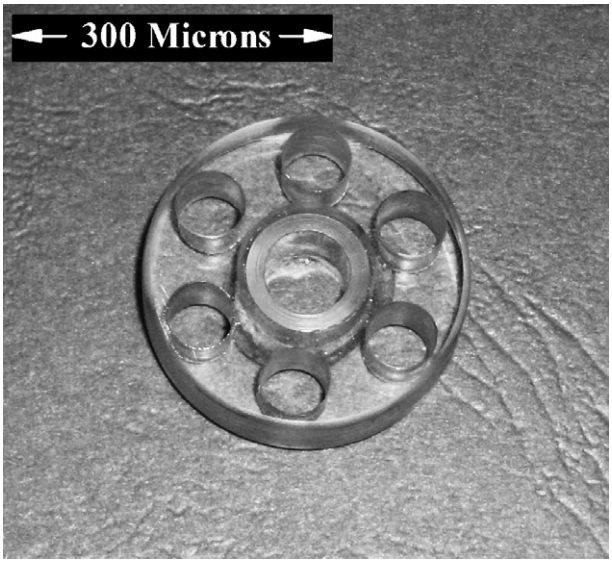

Fig. 2(c). Microscopic view of a multi-holed baffle plate fabricated using the laser ablation micromachining technique.

assembly. The access channels for the fuel and oxidizer streams are also visible. Fig. 2(c), on the other hand, illustrates the microscopic view of the multi-holed baffle plate for a prototype having smaller baffle holes and a larger fuel hole than that of the standard (base) geometry.

2.2. Experimental set-up and procedure

Experiments were conducted in a set-up (Fig. 3) consisting of: (i) the micro-reactor model described above, (ii) a closed-loop flow circuit, and (iii) the micro-PIV system. The flow circuit included a 10^{-3} m^3 fluid reservoir (tank), a control valve, a flow meter, a set of two syringe pumps (one each for the fuel and oxidizer streams, respectively) and a series of connecting tubes. The circuit eliminated the need for large quantities of the working fluid.

The micro-PIV system (Fig. 4) comprised a Quantel TWINS B double pulse Nd:YAG laser system ($2\times$ 380 mJ at 532 nm), an inverted microscope (Nikon Eclipse TE2000-U), a Dantec HiSense 80C60 CCD camera with an array size of 1279×1023 pixels, a camera integration package, fibre optic links, a high precision three-axis motorized stage (AS3000i/3500), a high speed data acquisition unit, and the Dantec *Flow-Manager* software.

The micro-PIV technique employed in this study has several advantages over the conventional particle image velocimetry (PIV) technique, making it the ideal tool for flow measurements in microfluidic devices. In the conventional PIV method, the flow domain is seeded by neutrally buoyant particles and a measurement plane is defined by a laser light sheet. The light scattered from the particles crossing the measurement plane is then captured by a CCD camera for analysis of the velocity and shear stress distributions. It is impossible to implement this configuration in microfluidic devices where the physical space is limited. To resolve this problem, in the micro-PIV approach the camera and the laser illumination are introduced through the inverted microscope via the fibre optic links. Unlike the standard PIV, volume illumination is used, hence, the numerical aperture of the microscope objective defines the measurement plane. The combination of the volume illumination and microscope allowed us to achieve focal depths ranging between 2 and 45 μm whereas the smallest focal depth achievable by the standard PIV is about 1 mm. As a result, with a nominal focal depth of 10 μm, 30 measurement planes were typically captured across the 300 μm diameter of the reactor model. The spatial resolution in each plane, defined by the size of the interrogation window, was 120×40 pixels corresponding to an area of 20×6.7 μm^2. The interrogation windows were overlapped by 50% according to the Nyquist sampling criterion to maximize the amount of information extracted. This yielded a velocity vector spacing of 10 μm in the stream-wise direction and a 3.35 μm spacing in the span-wise direction.

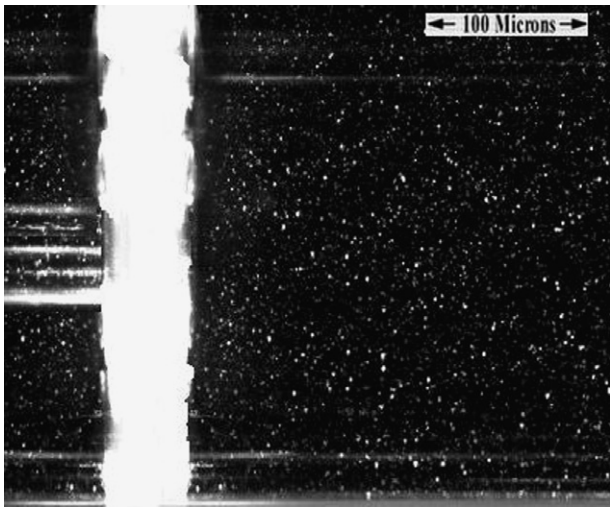

Fig. 4. A typical micro-PIV recording enhanced by the Overlapping method. The vertical white band in the picture is the baffle plate, which is not transparent to the laser light due its surface finishing.

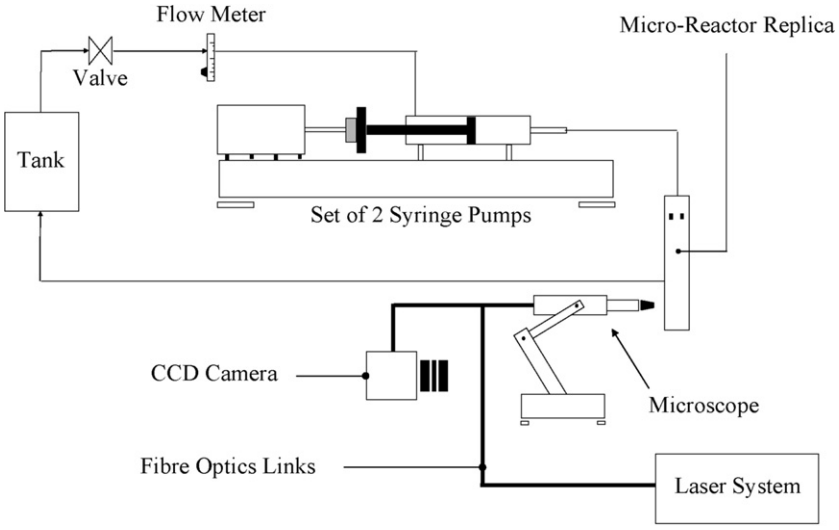

Fig. 3. Physical configuration of the experimental set-up.

Table 1
Test matrix

Set	Re[a]	Geometry
1	100	Standard geometry, no baffle plate
2	100	Standard geometry
3	100	Standard geometry except $d_1 = 30$ μm
4	100	Standard geometry except $d_1 = 10$ μm
5	100	Standard geometry except $d_2 = 30$ μm
6	100	Standard geometry except $d_2 = 70$ μm
7	100	Standard geometry except $R_1 = 105$ μm
8	300	Standard geometry

[a] Based on D (reactor diameter).

The seed particles were 700 nm red fluorescent polystyrene micro-spheres ($\rho = 1050$ kg/m^3) with a response time of 5×10^{-9} s. The particles were produced and packaged by the Duke Scientific Corporation as aqueous suspensions with 1% solids. Because of relatively high velocities used in the experiments (≈0.3 m/s) the effect of Brownian motion of seed particles was negligible.

To overcome the problem of low particle density in the Micro-PIV recordings (this is often referred to as "low image density" or LID in the literature), we employed the "Overlapping" method[1] (Nguyen and Wereley, 2002) in which nine pairs of PIV recordings were overlapped to artificially obtain an enhanced high particle density image pair for cross-correlation. Fig. 4 illustrates a micro-PIV recording enhanced by the overlapping method. Note that because of low Reynolds numbers, the laminar flow in our set-up can be considered as steady state during the data acquisition, hence, justifying the use of the Overlapping method. The method has also the added advantage of relatively high signal-to-noise ratio, which renders the vector validation post-processing unnecessary.

Experiments were carried out across each measurement plane and were repeated systematically at a fixed flow rate for various combinations of the fuel feed tube and baffle plate geometries (see Table 1). The overall flow rate was maintained at a rate to provide a nominal Re of 100. The Re number was defined based on the overall reactor diameter (D) and the mean velocity over its full cross-sectional area. The flow rate through the central tube of the model reactor was set to 5% of that fed through the annular space by adjusting the flow ratio between the relevant syringe pumps. The split ratio of 5% was chosen to approximate the fuel/air ratio of the methane/oxygen mixture in the actual reactor. The gathered data were digitized by a frame grabber board and then exported to the *Flow-Manager* software by which the velocity vector maps were quantified. Mixing efficiency was examined in terms of the size and strength of the high/low velocity regions and recirculation zones near the outlet of the central tube (i.e., fuel inlet tube in the actual reactor).

To maintain the similarity between the replica and the actual reactor, the Re number of the flow in the replica was kept at the same level as that in the actual reactor ($Re \approx 100$). Since both systems have identical dimensions and operate with similar flow rates, then the ratio of the density to viscosity for the replica $(\rho/\mu)_{rep}$ has to be equal to that of the actual reactor $(\rho/\mu)_{act}$. Considering that the real system operates with a mixture of methane and oxygen while water is the preferred option for the replica, the dynamic viscosity of water had to be adjusted to maintain the ρ/μ ratio. This was achieved by adding glycerin to water. As a result, the standard working fluid in this study was a mixture of 98 wt% water and 2% glycerin. The mixture was seeded with 1 μm orange florescent polystyrene particles for PIV measurements. A 0.1 wt% mixture of NaI with a sodium-based stabilizer ($Na_2S_2O_3$) was also added to the working fluid to match its refractory index with that of glass. This was to enhance the signal quality of the measurements.

3. Results and discussion

Fig. 5(a) illustrates a typical velocity vector map obtained from the first set (set 1, see Table 1) of experiments for a model reactor without the baffle plate but otherwise a standard geometry (i.e., co-axial jet). This particular figure shows an axial plane view of the region near the central inlet tube. As can be seen, owing to greater velocities of the fluid jets in the annular space, velocity profiles close to the outlet of the central tube exhibit steep gradients with minimums not only at vessel walls but also along the axis of symmetry. These profiles, however, quickly vanish and replaced by typical laminar flow

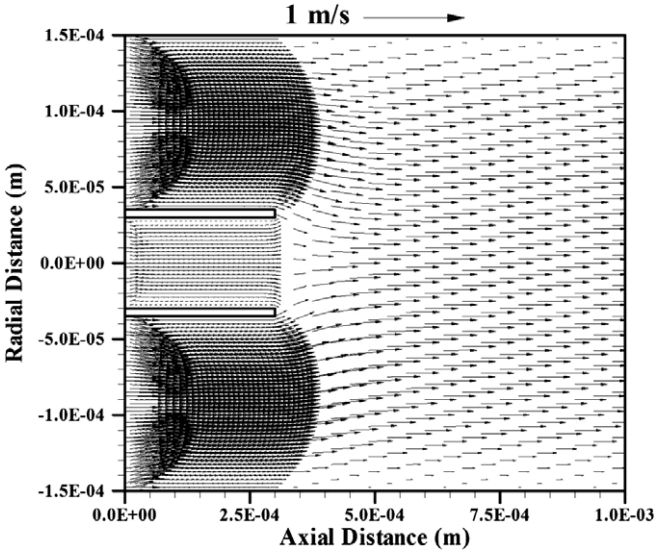

Fig. 5(a). The velocity vector map for a model reactor without the baffle plate.

[1] An alternative way of resolving the LID problem is to use the so-called "ensemble correlation" method (Nguyen and Wereley, 2002) using a much higher number of image pairs (typically 100). However, this approach was found to be beyond our capabilities and was not employed.

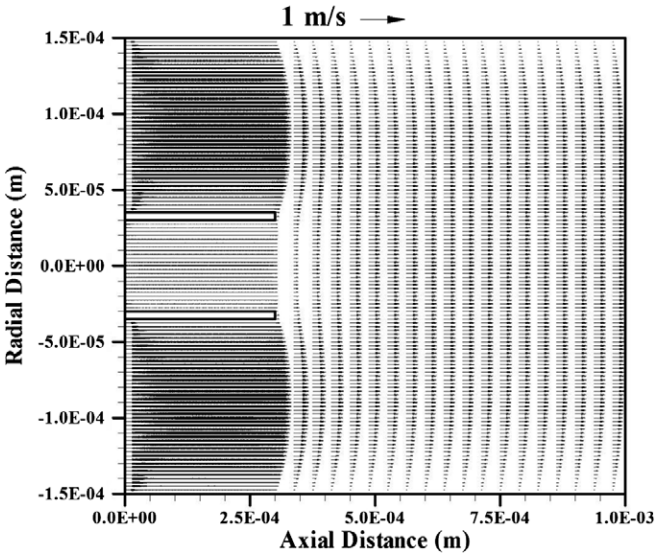

Fig. 5(b). The radial distribution of the axial velocity for the vector plot shown in Fig. 5(a).

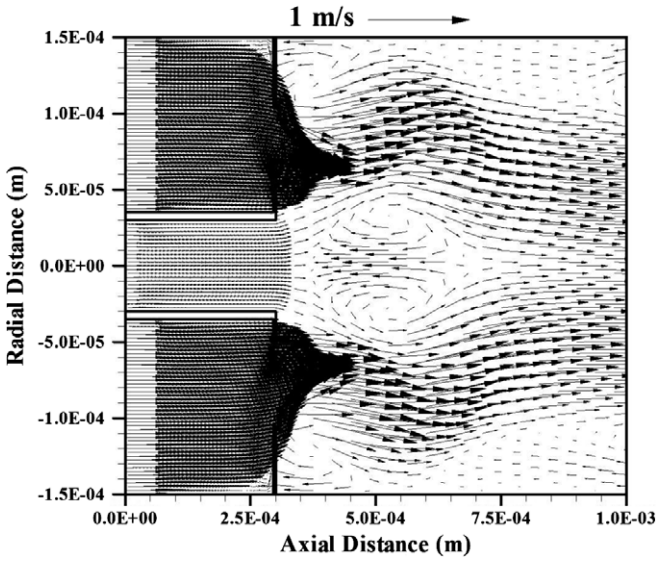

Fig. 6(a). The velocity vector map for a model reactor with the standard geometry (Fig. 1).

parabolic velocity profiles at downstream locations greater than two reactor diameters (i.e., 600 μm).

There are also several unusual flow structures on the far left hand side of Fig. 5(a) although they do not seem to have any significant impact on the flow passing through the baffle holes. These structures which are also observed in a number of other cases presented in Figs. 6–13, are caused by fluid particles which are trying to turn at the base of the T-piece formed by the main channel and the oxidizer access channels (see Fig. 2(a)). However, some of these fluid particles that are coming from the oxidizer access channels are unable to make a complete 90° turn and, as a result, develop a radial velocity component leading to the formation of the observed structures. If this hypothesis is true, there should be no sign of the unusual flow structures in a plot of the radial distributions of the axial velocity. This, as depicted in Fig. 5(b), is indeed the case.

Fig. 6(a) shows a velocity vector map obtained from the second set of experiments (set 2) for the standard geometry. Similar to Fig. 5 only the regions close to the central tube are shown. Clearly, there is a dramatic difference between the flow field shown in Fig. 6 and that of the simple co-axial jet configuration shown in Fig. 5. Unlike the previous case, there is a relatively large reverse flow region, accompanied by two recirculation zones, near the central tube outlet. As shown in Fig. 6(b), the recirculation zones are formed as a result of the outward flow of fluid particles in radial direction caused by the formation of an stagnation point immediately in front of the central tube. The existence of the reverse flow and recirculation zones in the vicinity of the central tube implies that the flow structure in this region must be dominated by convective effects (i.e., bulk flow). This greatly enhances the mixing of the fluid streams when compared with the simpler case of the co-axial jet for which the mixing phenomenon is dominated

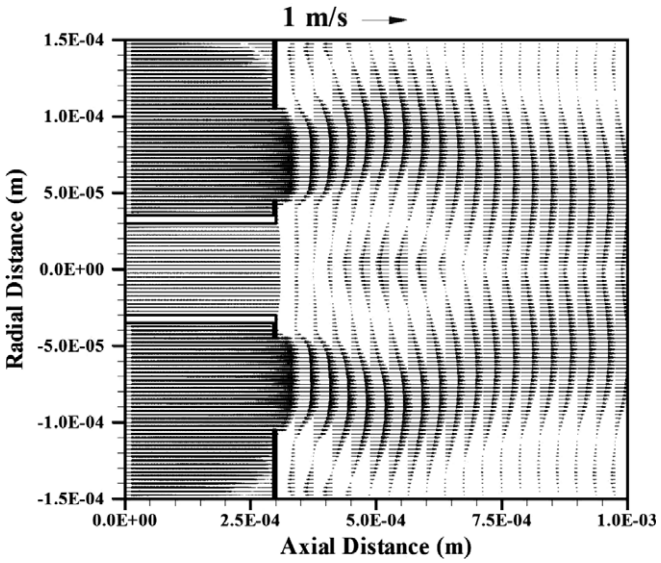

Fig. 6(b). The radial distribution of the axial velocity for the vector plot shown in Fig. 6(a).

by the time scale for molecular diffusion (Woodfield et al., 2003).

As mentioned before, apart from the first two sets of experiments, several other sets of tests were carried out to closely examine the impact of the reactor geometry on the mixing phenomenon. On this basis, the third and fourth sets of experiments (sets 3 and 4) were conducted to investigate the effect of reducing the size of the central tube diameter on the recirculation/reverse flow zones in front of the central tube. The results have been summarized in Figs. 7 and 8 for cases with 50% and 83% reduction in the central tube diameter, respectively.

Evidently, as the diameter of the central tube is decreased, the recirculation/reverse flow zones disappear

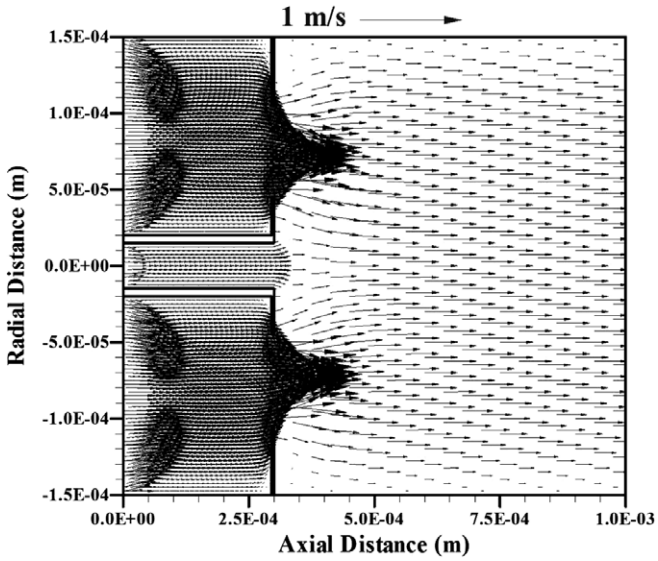

Fig. 7. The velocity vector map for a model reactor with a central tube diameter reduced by 50% from that of the standard geometry ($d_1 = 30$ μm).

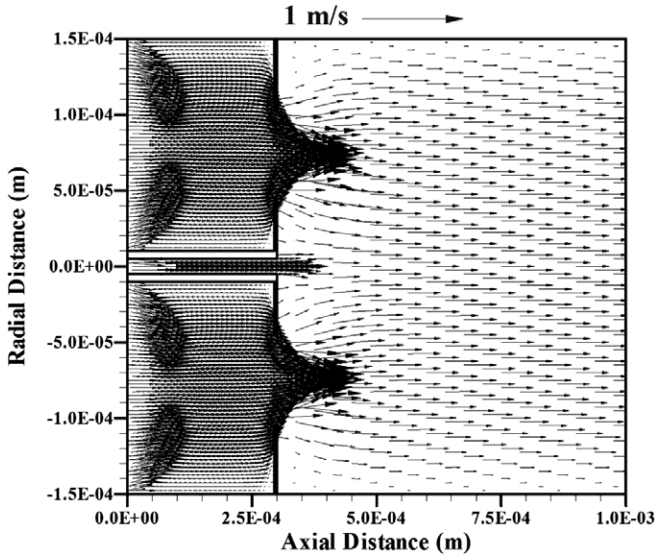

Fig. 8. The velocity vector map for a model reactor with a central tube diameter reduced by 83% from the standard geometry ($d_1 = 10$ μm).

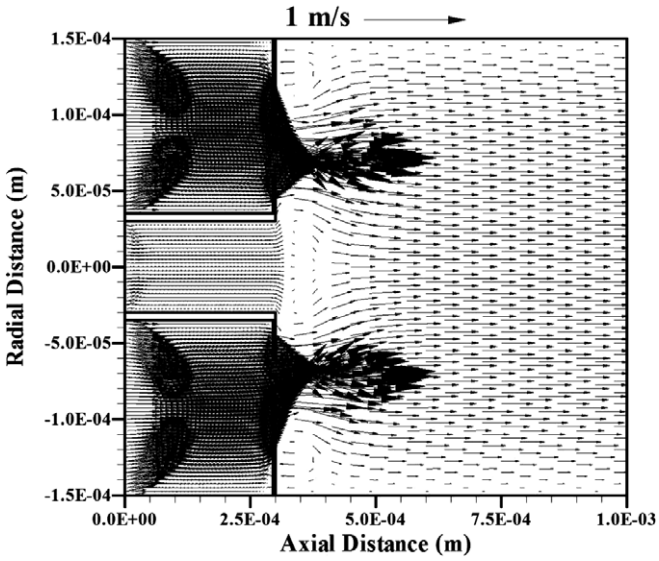

Fig. 9. The velocity vector map for a model reactor with smaller baffle holes ($d_2 = 30$ μm) otherwise standard geometry.

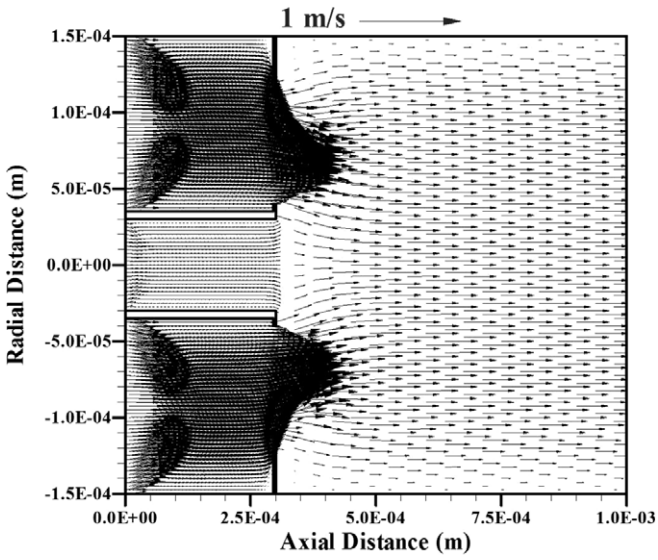

Fig. 10. The velocity vector map for a model reactor with larger baffle holes ($d_2 = 70$ μm) otherwise standard geometry.

(see Figs. 7 and 8), implying that the enhancement to mixing achieved with the standard geometry is diminished. This can be assigned to the fact that the reduction of the central tube diameter increases the velocity of the co-axial jet exiting from the central tube. This increased velocity associated with the higher momentum of the jet pushes the stagnation point further and further away from the central tube outlet. For certain central tube sizes like those shown here, the jet momentum becomes so high that it significantly reduces the entrainment of the fluid jets exiting the baffle holes and, thereby, prevents the formation of the reverse flow region. As a result, the reverse/recirculation zones fade away and the flow structure becomes very much similar to that of a simple co-axial jet configuration having no baffle plate.

The influence of the baffle plate geometry on the flow structure and mixing phenomenon near the central tube outlet was examined in experimental sets 5–7. While the impact of the baffle hole diameter on the flow structure was studied in sets 5 and 6, the effect of baffle hole radial location was examined in the seventh set of experiments.

Figs. 9 and 10 illustrate the resulting flow and mixing pattern for smaller and larger baffle hole diameters, respectively. Apart from the hole diameter all other dimensions are identical to those of the standard geometry. As Fig. 9 indicates, for the smaller hole configuration the velocity

and momentum through the holes are greatly increased causing a notable reduction in the extent of the recirculation and reverse flow zones. Compare with the standard geometry (Fig. 6), the stagnation point in front of the central tube in Fig. 9 has moved upstream towards the tube outlet. Also there is a pair of counter rotating recirculation zones near the junction between the baffle plate and the reactor wall. Similar zones also exist for the standard geometry (Fig. 6) although their sizes appear to be different from those shown in Fig. 9.

In the case of the larger baffle hole configuration shown in Fig. 10, the impact of the hole size seems to be more pronounced as the stagnation point and reverse flow/recirculation zones disappear altogether. The implication of this finding is that the standard geometry provides an optimum configuration for the flow rates considered in the present study. As such, any deviation from the base geometry causes significant departure from the flow structure and mixing patterns observed in Fig. 6.

Fig. 11 summarizes the results obtained from the seventh set of experiments in which the effect of baffle hole radial location was examined. In this particular figure, the baffle holes have been moved outwards in radial direction by as much as 30 μm (i.e., $R_1 = 105$ μm). Only half of the flow domain is shown in Fig. 11 so a comparison can be made with the base case. As can be seen, once again a relatively small change in the baffle geometry creates a dramatic change in the flow structure. In particular, the extent and strength of the reverse flow/recirculation zones have considerably increased indicating that having baffle holes close to the reactor wall help to enhance the overall mixing. Therefore, the standard geometry can be optimized by moving the baffle holes outwards in the radial direction.

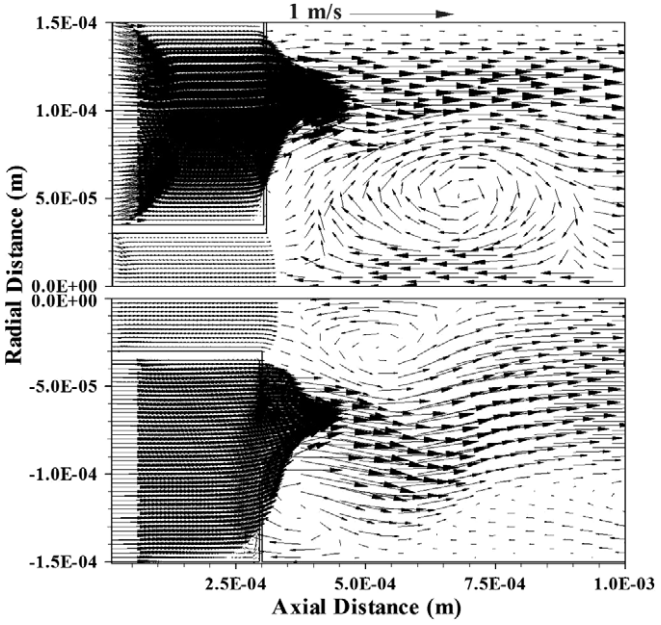

Fig. 11. The velocity vector map (top half of the figure) for a model reactor with baffle holes in a different radial location ($R_1 = 105$ μm) from that of the standard geometry. For comparison, the vector map of the standard geometry has been plotted in the bottom half of the figure.

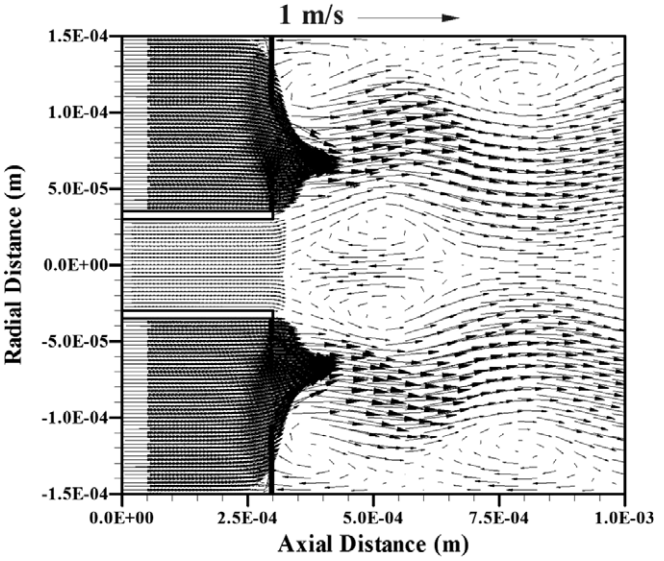

Fig. 12. The velocity vector map for a model reactor with standard geometry at $Re = 300$.

The final set of experiments was dedicated to study the effect of Reynolds number. This was motivated by the fact that in real situations the micro-reactor may be operated over a range of flow rates all with a similar fuel/oxidizer ratio. As with the other sets of experiments the *Re* number (Table 1) was defined based on the overall reactor diameter (D) and the mean velocity over its full cross-sectional area. The *Re* in the final set of experiments was varied from the base value of 100 to 300 at increments of 50. The summary of results for a *Re* number of 300 at a region close to the central tube and baffle plate is depicted in Fig. 12. As shown, the reverse flow/recirculation zone immediately in front of the central tube, both in terms of size and velocity magnitude, are very similar to those of the base case for a *Re* of 100 (Fig. 6). However, the recirculation zones near the reactor wall appear to be larger.

There is also a new reverse flow/recirculation zone downstream from the first one in front of the central tube (Fig. 13). While in terms of the velocity magnitude, the second reverse flow/recirculation zone does not seem to be as strong as the first one, its size is certainly much bigger. A closer examination of the results for other Reynolds numbers shows very similar flow features. This implies that an increase in *Re* number results in a general expansion of the flow field and mixing patterns in the axial direction, leading to an overall enhancement of the mixing phenomenon. It must be highlighted, however, not all flow features expand in proportion to *Re*. This is in contrast to many other types of laminar flow, such as, laminar confined jets (Woodfield et al., 2003), laminar free jets (Pai and Hsieh, 1972), and sudden expansion duct flow (Macagno and Hung, 1967) where the flow features expand linearly with the Reynolds number. The difference can be partly assigned to the combined effects of the convective and diffusional

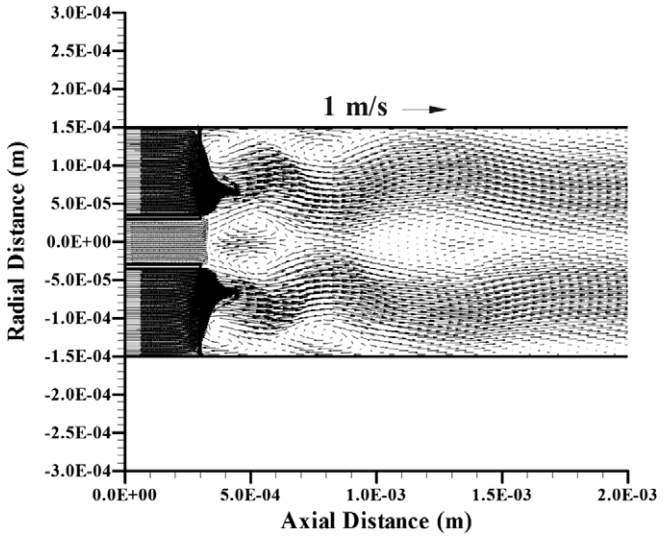

Fig. 13. The velocity vector map similar to that shown in Fig. 12 but with a lower magnification showing a larger portion of the flow field.

transports in the cross-stream direction, particularly in regions close to the baffle plate and central tube. Such combined effects do not generally exist in other types of laminar flows. In the case of laminar confined jets, for example, the cross-stream flow is dominated by diffusional transport while the transport in stream-wise direction by inertial forces (i.e., convective effect).

4. Conclusions

The following conclusions can be drawn from the experimental results presented in this paper:

- The multi-hole baffle plate configuration considerably enhances the mixing performance of the reactant stream in the micro-reactor investigated as part of the present study.
- The baffle plate and central tube geometries were found to have dramatic impacts upon the flow structure and mixing patterns. As such, the reactor geometry has to be optimized to achieve the desirable mixing performance.
- For the range of *Re* studied here, the optimum reactor geometry seems to be the one having similar central tube and baffle hole diameters. The optimum radial location for baffle holes appear to be half way between the stream-wise axis and the reactor wall (i.e., $D/4$).
- Increasing the Reynolds number for the optimum reactor geometry enhances the mixing performance.

Acknowledgements

The authors wish to acknowledge the financial support provided to him by the University of Newcastle (Australia), the Vienna University of Technology (Austria), and the Australian Research Council through the Linkage-Infrastructure Scheme, grant number: LE0230569.

References

Choi, H.S., Katsumoto, Y., Nakabe, K., Suzuki, K., 2002. An experimental investigation of mixing and combustion characteristics on the can-type micro combustor with a multi-jet baffle plate. Fluid Mechanics and Its Applications – Turbulent, Mixing and Combustion 70, 367–375.

Ehrfeld, W., Hessel, V., Loww, H., 2000. Microreactors: New Technology for Modern Chemistry. Wiley-VCH, New York.

Fletcher, P.D., Haswell, S.J., Pombo-Villar, E., Warrington, B.H., Watts, P., Wong, S.Y.F., Zhang, X., 2002. Micro reactors: principles and applications in organic synthesis. Tetrahedron 58, 4735–4757.

Macagno, E.O., Hung, T., 1967. Computational and experimental study of a captive annular eddy. Journal of Fluid Mechanics 28, 43–64.

Nguyen, N.T., Wereley, S., 2002. Fundamentals and Applications of Microfluidics. Artech House.

Pai, S.I., Hsieh, T., 1972. Numerical solution of laminar jet mixing with and without free stream. Applied Scientific Research (The Hague) 2 (1), 39–62.

Penner, S.S., 2004. Steps towards the hydrogen economy. Energy 31 (1), 33–43.

Sobek, D., Senturia, S.D., Gray, M.L., 1994. Technical Digest of the IEEE Solid State Sensor and Actuator Workshop. pp. 260–263.

Tiggelaar, R.M., Loeters, P.W.H., van Male, P., Oosterbroek, R.E., Gardeniers, J.G.E., de Croon, M.H.J.M., Schouten, J.C., Elwenspoek, M.C., van den Berg, A., 2004. Thermal and mechanical analysis of a micro-reactor for high temperature catalytic gas phase reactions. Sensors and Actuators A 112, 267–277.

Wegeng, R.S., Pederson, L.R., TeGrotenhuis, W.E., Whyatt, G.A., 2001. Compact fuel processors for fuel cell powered automobiles based on microchannel technology. Fuel Cell Bulletins 28, 8–13.

Winter, J.C., 2004. The hydrogen energy economy: an address to the world economic forum 2004. International Journal of Hydrogen Energy 29, 1095–1097.

Woodfield, P.L., Nakabe, K., Suzuki, K., 2003. Numerical study for enhancement of laminar flow mixing using multiple confined jets in a micro-can combustor. International Journal of Heat and Mass Transfer 46, 2655–2663.